NRC Research Press

ARTICLE

Multilayer graphene synthesized using magnetron sputtering for planar supercapacitor application

Mihnea Ioan Ionescu, Xueliang Sun, and Ben Luan

Abstract: This study reports the direct preparation of graphene-based films using magnetron sputtering of graphite target. The nanomaterial was deposited at a low temperature of 620 °C on silicon wafers and on metallic foils including aluminum. The films were used in fabrication of supercapacitors with a planar geometry. Electrochemical characterizations demonstrated that the films produced showed nearly ideal electrical capacitive behavior. The maximum capacitance obtained from cyclic voltammetry analysis was 325 F/g for a scan rate of 1 mV/s. The device is capable of delivering an energy density of 13.9 Wh/kg at a very high power density of 50 000 W/kg for ultrafast scan rate of 1000 mV/s. The graphene nanomaterial electrode retains the electrochemical stability over a large number of charge-discharge cycles.

Key words: nanomaterials, graphenes, magnetron sputtering, supercapacitor.

Résumé : La présente étude décrit la fabrication directe de films à base de graphène à l'aide de la pulvérisation magnétron d'une cible en graphite. Le nanomatériau a été déposé à basse température, soit 620 °C, sur des plaquettes de silicium et sur des feuilles métalliques contenant de l'aluminium. Les films ont été utilisés dans la fabrication de supercondensateurs de forme géométrique plane. Les caractérisations électrochimiques ont montré que les films produits présentaient un comportement électrique capacitif presque parfait. La capacitance maximale obtenue par analyse voltammétrique cyclique était de 325 F/g pour une vitesse de balayage de 1 mV/s. Le dispositif est capable de délivrer une densité d'énergie de 13,9 Wh/kg à une puissance massique très élevée de 50 000 W/kg et pour une très grande vitesse de balayage de 1000 mV/s. L'électrode en nanomatériau de graphène reste électrochimiquement stable pendant un nombre important de cycles charge-décharge. [Traduit par la Rédaction]

Mots-clés : nanomatériaux, graphènes, pulvérisation magnétron, supercondensateur.

Introduction

Nanostructured carbon materials, including nanotubes and graphene sheets, have attracted tremendous interest over the past few years because of their outstanding electrical and mechanical properties.[1–4] Graphene and few layer graphene sheets are atom-thick layers of sp^2 bonded carbon atoms that present large in-plane conductivity, are lightweight, and have an enormous surface area.[5] Graphene-based films are expected to play an important role in the development of portable electronics, power tools, hybrid electric vehicles, and grid support applications.[6]

A key factor for the industrial production of graphene is to find cost-effective technologies that permit large area synthesis of graphene at low temperatures. A low-temperature process is essential for the silicon-based electronic industry, while direct synthesis of graphenes on different substrate types and on materials with a low melting point such as aluminum, glass, and plastics is highly desirable.[7]

Up to now, two methods have been used to synthesize large area graphene-based films: the oxidation and chemical reduction of graphite[8,9] and the thermal chemical vapor deposition (CVD) on metal surfaces.[10–12] The first method requires complicated liquid waste treatments and time-consuming procedures, while the latter method is restricted to a high deposition temperature of around 1000 °C. Plasma CVD is a versatile technique that offers high reaction rates, short deposition times, and lower growth temperatures compared with conventional thermal methods. However, the previous studies have reported high temperatures and high plasma discharge powers for graphene synthesis.[13–15]

Magnetron sputtering is a physical vapor deposition method that relies on the bombardment by energetic ions of a target made of the material to be deposited. The ions are primarily generated by the ionization of a working gas under an applied voltage. During bombardment, the atoms of the target material are ejected and then float and condense on a substrate that is placed on the line of sight of the target.[16] Unlike other methods, sputtering does not involve chemical interaction among the species resulting from the deposition process. The energy of the ejected atoms can compensate traditional energy sources, such as heating, that are required to promote the film growth and to improve its characteristics. Sputtering can be used to deposit quality films at moderate temperatures and even at room temperature. These factors enable compatibility of the deposition method with a wide variety of substrates and make sputtering a technology of choice for various thin film applications. Nevertheless, few studies on nanostructured carbon materials obtained using magnetron sputtering[17–19] and even fewer for graphene synthesis[20] have been reported so far. To the best of our knowledge, studies of graphenes synthesized using magnetron sputtering on silicon and metallic foils have not been reported.

Herein, we report an efficient, rapid, low-cost, and scalable approach for the synthesis of multilayer graphene sheets by using

Received 19 June 2014. Accepted 13 August 2014.

M.I. Ionescu and B. Luan. Automotive and Surface Transportation, National Research Council Canada, London, ON N6G 4X8, Canada.
X. Sun. Department of Mechanical and Materials Engineering, The University of Western Ontario, London, ON N6A 5B9, Canada.
Corresponding author: Mihnea Ioan Ionescu (e-mail: mihnea.ionescu@nrc-cnrc.gc.ca).

This article is part of a Special Issue conceived to celebrate the centennial of the first research publication emanating from the Department of Chemistry at The University of Western Ontario and to highlight the chemical research now being performed by faculty and alumni.

Fig. 1. (*a*) Photograph of graphene-based film floating on deionised water after etching away the substrate. (*b*) Prototype of the planar supercapacitor and (c) the schematic diagram of the device.

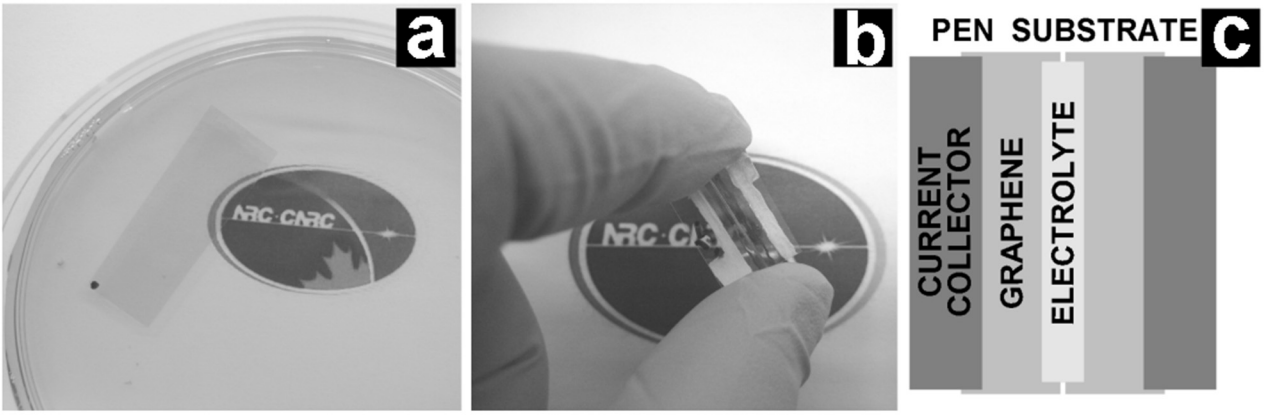

magnetron sputtering of graphite target. The deposition was performed at a temperature of 620 °C on different substrates including aluminum foil.

The graphene-based films were used as electrodes in the fabrication of supercapacitors with a planar geometry. The device architecture offers an enhanced interaction of the electrolyte with carbon layers, leading to a good utilization of the high specific surface area offered by graphene films.[21] These are reflected in an excellent capacitive performance and stability over a large number of charge–discharge cycles. The design has the potential of full integration into the manufacturing process of printable electronics and energy storage devices.

Experimental details

Synthesis of graphene

Graphene layers were synthesized by RF magnetron sputtering (13.56 MHz) in a vacuum deposition system (model FLR-900H, Plasmionique Inc., Canada), using a pure carbon target (Kurt J. Lesker, USA) with a diameter of 5.08 cm. Different substrates such as silicon wafers (University Wafer, USA) and Cu, Ni, Al metallic foils (Sigma-Aldrich, USA) were placed on a substrate holder heated from below by an electronically controlled resistive heating element. The temperature was measured and controlled using thermocouples. The first thermocouple was placed in contact with the substrate. The second thermocouple was placed under the substrate holder and calibrated to indicate the temperature of the substrate. This arrangement minimizes errors in temperature reading when plasma is ignited. In a typical experiment, the substrate was heated to 620 °C in argon atmosphere, after allowing 10 min for temperature equilibration. The argon gas was introduced in the deposition chamber with a flow rate of 14 sccm (standard cubic centimeters per minute) maintaining a pressure of 2 Pa. The sputtering process was performed for 10 min, using an RF plasma power of 100 W and a target to substrate distance of 150 mm. After deposition, the reactor was allowed to cool down under vacuum before exposure to air.

Supercapacitor fabrication

Graphene films were transferred to polyethylene naphthalate PEN substrates (Delta Scientific, Canada) after etching away the copper foil in an aqueous solution of $FeCl_3$ (1 mol/L) and washing with deionized water (Fig. 1*a*). Capacitors were fabricated by scratching the graphene layer with a blade to form two graphene electrodes separated by a 0.7 mm gap, and painting the polymer electrolyte over the graphene electrodes. The total area of graphene exposed to electrolyte was 1.1 cm × 0.13 cm = 0.14 cm^2. The polymer electrolyte was prepared by adding poly(vinyl alcohol) (PVA) and phosphoric acid (1.6 g) in deionized water (2 g PVA in 20 mL H_2O) and stirring the mixture at 80 °C until a transparent gel was obtained. The current collectors were finalized by painting electrical contacts over the graphene electrodes using a conducting silver paste (Leitsilber 200 Silver Paint, Ted Pella Inc., USA). A prototype supercapacitor in a planar geometry based on graphene current collectors and its schematic diagram are presented in Figs. 1*b* and 1*c*.

Characterization methods

The samples were characterized by Raman spectroscopy (Horiba Scientific, LabRAM HR 800, with an incident laser beam of 532.4 nm) without removing or etching the substrate. Field emission scanning electron microscopy (FE-SEM, Hitachi S-4800, operating at an accelerating voltage of 5 kV) was performed after the as grown film was transferred to Si substrate. Cyclic voltammetry (CV) and galvanostatic charge–discharge measurements were performed using the electrochemical interface Solartron SI-1287. The specific capacitance and cyclic stability of devices were evaluated in a two-electrode configuration.

Results and discussion

The Raman spectra of carbon nanomaterial synthesised on Si wafer and on metallic foils present four major peaks, representing D, G, 2D, and D+G bands (Fig. 2*a*). The peak, found at ~1587 cm^{-1} and referred to as the G band, corresponds to the optical phonon modes of E_{2g} symmetry in graphite and indicates the existence of well graphitized graphene-based films.[22,23] The D band, positioned at 1343 cm^{-1} and the shoulder D′, found at 1610 cm^{-1} in the G band profile, are associated with the disordered state of the sp^2 hybridized material that could result from defects, substitutional atoms, stress induced by the cooling process, finite size, or orientation of graphene domains.[24,25] While the D′ band cannot be observed in significantly disordered carbons such as carbon black, it appears in the graphite-like carbon materials with relatively low disorder, such as microcrystalline graphite and glassy carbon.[26] At higher wavenumbers, the spectra of all samples reveal the second order of Raman bands associated with 2D band around 2684 cm^{-1}, and that of the D + G band at 2936 cm^{-1}. The presence of the D′ band and of 2D and D+G combinational Raman modes prove that the deposited film is formed by well-oriented few-layer graphene domains.[27]

The general aspect of the Raman spectra of graphene films grown on Si wafers and on metallic foils presents the same characteristics regardless of substrate used for nanomaterial synthesis. The spectra present no major shifts of the main peaks or dramatic differences in the intensity ratio I_D/I_G of the D and G bands, which estimate the concentration of defects in graphene.

Fig. 2. (*a*) Raman spectra of carbon nanomaterial synthesised on different substrate types. Representative SEM images of carbon nanomaterial at (*b*) low magnification and (*c*) high magnification.

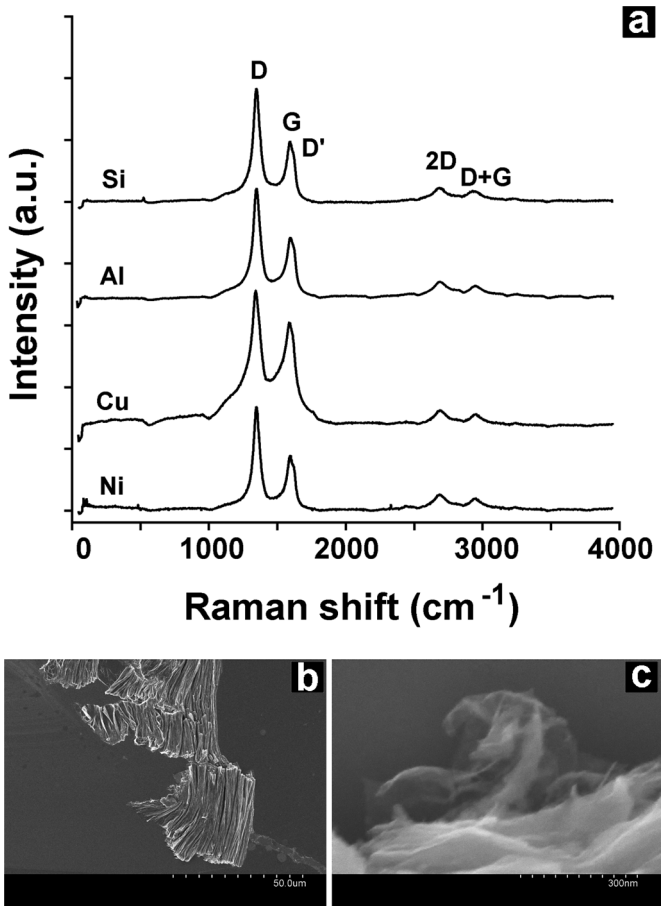

These observations suggest that the process of graphene formation differs from the growth mechanism of graphene on metal substrates, especially for nickel and copper substrates. For these materials the mechanism is based on graphene segregation on the metallic surface realized at high temperatures and is determined by the carbon solubility in the metal substrates.[28]

Although our study does not focus on the growth mechanism of graphene synthesized by magnetron sputtering, the process could be related to the growth mechanism proposed by Hiramatsu et al.[29] Their study suggested that carbon species condense to form nano-islands that develop into nano-flakes with disordered orientation and eventually grow into a continuous wall-like structure. A similar growth mechanism could be attributed to this study, since no metal catalyst has been used. For magnetron sputtering of carbon on heated substrates, carbon clusters are formed during the transport of sputtered atoms from the target zone to the substrate. When in contact with the heated substrate, the carbon clusters rearrange and form the graphene domains on the substrate surface with less influence from the substrate type. The size and the number of such clusters could be strongly dependent on the collision frequency and transport time. These factors are influenced by different growth parameters, such as deposition pressure, plasma power, flow rate of the carrier gas, and distance of substrate from target. In addition, the quality of graphene could be improved by increasing the substrate temperature. However, even at low temperatures, graphene can be obtained on different types of materials and on substrates with low melting points, such as aluminum. Further elaboration to find details in the mechanism of graphene formation using magnetron sputtering of carbon on heated substrates is under investigation by our group. More experiments are also required to find the optimum atmosphere for growing high-quality graphene films. Although graphene can be grown using argon gas alone, the addition of hydrogen during the synthesis process is expected to improve the quality of the films, because hydrogen is known to selectively etch amorphous carbon defects.[30,31]

Raman spectra and SEM imaging have revealed almost identical characteristics for all samples regardless of material substrate. Due to these strong similarities, the following characterizations were conducted only for samples obtained on copper foil. The material obtained after etching away the foil has been transferred to Si wafers for observations. The film is uniformly deposited over large scale-lengths and can be scratched out of the substrate without destroying the film (Fig. 2*b*). The material exhibits crumpled and folded features typical to two-dimensional carbon nanosheets. At high magnification it is observed that the film is without visible defects or voids and is approximately 3 nm in thickness (Fig. 2*c*).

The graphene-based films obtained from etching away the Cu foil were transferred to flexible PEN substrates and used in the fabrication of supercapacitors with a planar geometry. Using a polymer gel electrolyte over the graphene electrodes facilitates the electrolyte to interact with graphene layers and to take advantage of their high surface area. The final devices based on planar architecture are robust, lightweight, thin, transparent, flexible, and can be realized using only printing techniques.

The electrodes of graphene have a total exposure area of 1.1 cm × 0.13 cm = 0.14 cm^2 and a measured mass of 0.107 μg determined by finding the mass (40.5 μg) of a graphene film with an area of 54 cm^2. The specific geometrical area of graphene electrodes of 133 m^2/g was evaluated from the mass and the geometrical area of electrodes. The number of layers in the graphene-based film used as electrode can be calculated knowing that the geometrical area of one graphene layer is 1310 m^2/g.[32] Therefore, the graphene based electrode has N = 1310 m^2/g/133 m^2/g = 9.8∼10 layers.

The electrochemical performances of the graphene-based devices were studied using cyclic voltammetry and galvanostatic charge–discharge. The CV scans were conducted in the range of 0–1 V at various scan rates from 1 to 1000 mV/s (Fig. 3*a*). The profiles of the CV curves are close to rectangular shape even at the ultrafast scan rate of 1000 mV/s, indicating the formation of an efficient capacitor with good electrical conductivity and fast electrolyte transfer to electrode. This behavior indicates good performances for fast charge–discharge applications.[33] The capacitance of the film was calculated from the CV curves according to the equation $Cs = (\int i \cdot dV)/m \cdot \Delta V \cdot S$, where Cs is the specific capacitance, $\int i \cdot dV$ is the integral area of the CV curve, m is the mass of active material, ΔV is the potential range, and S is the scan rate. Figure 3*b* shows the variation of the specific capacitance as a function of scan rates.

Graphene-based films retain 70% of their capacitance when the scan rate was increased from 1 to 100 mV/s and more than 50% for ultrafast scan rate of 500 mV/s. This suggests a good contact between the electrolyte and the active material and a good utilization of the high surface area offered by the graphene layers.[21]

The energy density $E = Cs \cdot (\Delta V)^2/2$ and power density $P = E/t$, were calculated at each scan rate, knowing that Cs is the specific capacitance, ΔV is the potential range, and t is the time to charge or discharge. For a low scan rate S = 1 mV/s, the energy density is 44.4 Wh/kg at a power density of 160 W/kg. For fast scan rate S = 1000 mV/s, the capacitor presents very good performances, being capable of delivering an energy density of 13.9 Wh/kg at a very high power density of 50 000 W/kg.

Galvanostatic charge–discharge curves were obtained at constant current densities of 1, 2.5, 5, and 10 A/g (Fig. 3*c*). The charge–discharge curves are close to a triangular shape with the discharge curves nearly symmetric with their corresponding charge coun-

Fig. 3. Electrochemical performance of graphene-based film planar supercapacitor. (*a*) CV curves at various scan rates. (*b*) The specific capacitance calculated from CV curves at different scan rates. (*c*) Galvanostatic charge–discharge curves at different current densities. (*d*) Capacitance retention versus the cycle number.

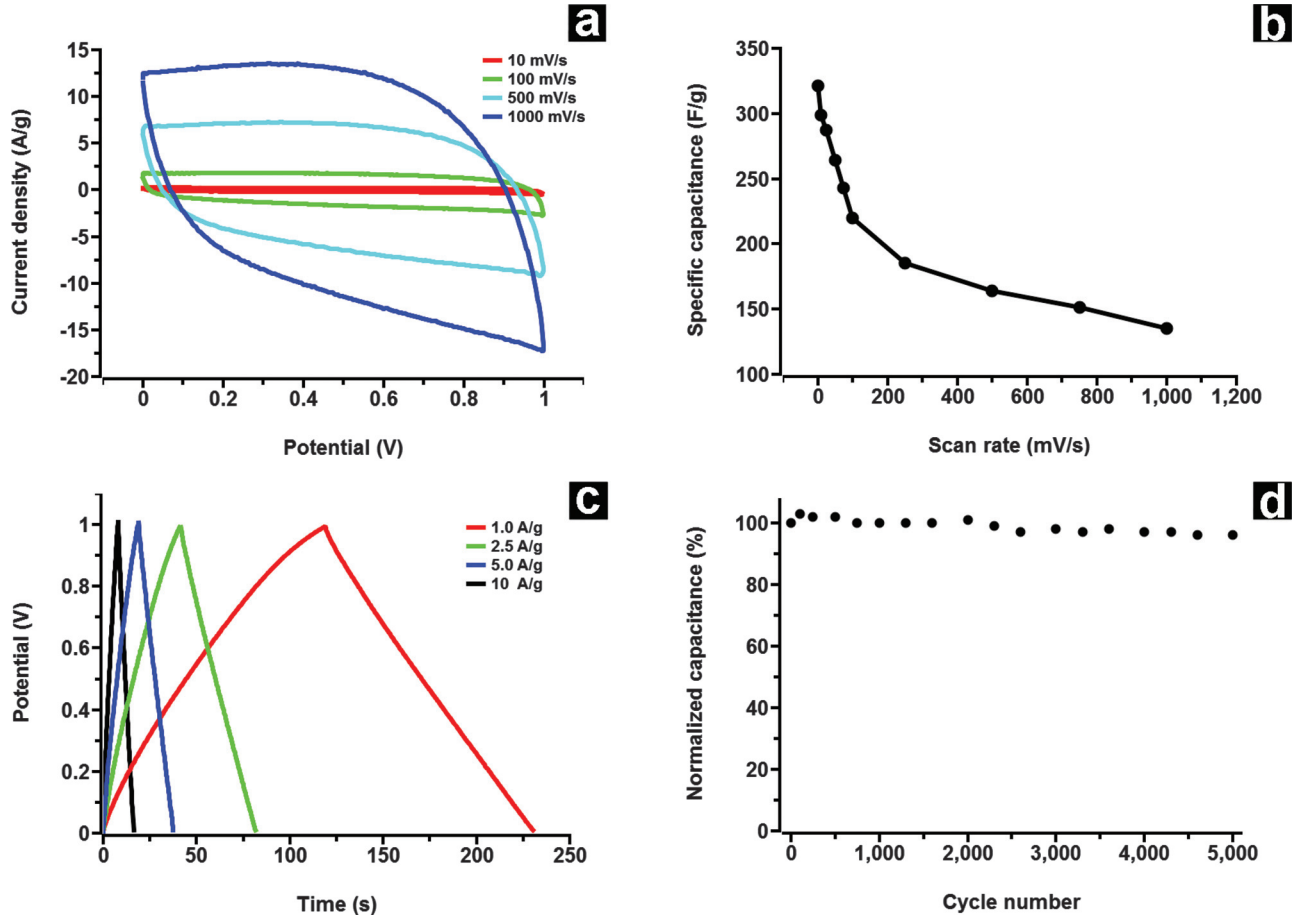

terparts, confirming good charge propagation across the graphene film electrodes and good electrochemical reversibility.[34]

The planar supercapacitor shows essentially negligible capacitance degradation after 5000 cycles (less than 5%), confirming that graphene nanomaterial retains good stability over a large number of charge–discharge cycles.

Conclusion

In conclusion, we present a simple method for fabricating graphene-based films at low temperatures on different substrates. The films were used in the fabrication of supercapacitors with a planar geometry, which efficiently facilitates the access of electrolyte ions in the active graphene material. Cyclic voltammetry analysis indicates a maximum capacitance of 325 F/g for 1 mV/s scan rate. At a very high power density of 50 000 W/kg and fast scan rate of 1000 mV/s, the device delivered an energy density of 13.9 Wh/kg. The graphene-based electrodes have an excellent electrochemical stability over a number of 5000 charge–discharge cycles.

The simple graphene-based capacitor architecture combined with the economical magnetron sputtering deposition method has the potential to lead to development of a new class of printable, flexible, and lightweight charge storage devices.

Acknowledgements

The authors gratefully acknowledge the National Research Council Canada (NRC) and The University of Western Ontario (UWO) for supporting this research.

References

(1) Dresselhaus, M. S.; Dresselhaus, G.; Charlier, J. C.; Hernández, E. *Phil. Trans. R. Soc. Lond. A* **2004**, *362*, 2065. doi:10.1098/rsta.2004.1430.
(2) Son, Y.-W.; Cohen, M. L.; Louie, S. G. *Nature* **2006**, *444*, 347. doi:10.1038/nature05180.
(3) Du, J.; Zhao, L.; Zeng, Y.; Zhang, L.; Li, F.; Liu, P.; Liu, C. *Carbon* **2011**, *49*, 1094. doi:10.1016/j.carbon.2010.11.013.
(4) Poot, M.; Van Der Zant, H. S. J. *Appl. Phys. Lett.* **2008**, *92*, 063111. doi:10.1063/1.2857472.
(5) Novoselov, K. S.; Geim, A. K.; Morozov, S. V.; Jiang, D.; Zhang, Y.; Dubonos, S. V.; Grigorieva, I. V.; Firsov, A. A. *Science* **2004**, *306*, 666. doi:10.1126/science.1102896.
(6) Su, D. S.; Centi, G. *J. Energy Chem.* **2013**, *22*, 151. doi:10.1016/S2095-4956(13)60022-4.
(7) Kim, J.; Ishihara, M.; Koga, Y.; Tsugawa, K.; Hasegawa, M.; Iijima, S. *Appl. Phys. Lett.* **2011**, *98*, 091502. doi:10.1063/1.3561747.
(8) Becerril, H. A.; Mao, J.; Liu, Z.; Stoltenberg, R. M.; Bao, Z.; Chen, Y. *ACS Nano* **2008**, *2*, 463. doi:10.1021/nn700375n.
(9) Eda, G.; Fanchini, G.; Chhowalla, M. *Nat. Nanotechnol.* **2008**, *3*, 270. doi:10.1038/nnano.2008.83.
(10) Li, X.; Cai, W.; An, J.; Kim, S.; Nah, J.; Yang, D.; Piner, R.; Velamakanni, A.; Jung, I.; Tutuc, E.; Banerjee, S. K.; Colombo, L.; Ruoff, R. S. *Science* **2009**, *324*, 1312. doi:10.1126/science.1171245.
(11) Kim, K. S.; Zhao, Y.; Jang, H.; Lee, S. Y.; Kim, J. M.; Kim, K. S.; Ahn, J.-H.; Kim, P.; Choi, J.-Y.; Hong, B. H. *Nature* **2009**, *457*, 706. doi:10.1038/nature07719.
(12) Bae, S.; Kim, H.; Lee, Y.; Xu, X.; Park, J.-S.; Zheng, Y.; Balakrishnan, J.; Lei, T.; Ri Kim, H.; Song, Y. I.; Kim, Y.-J.; Kim, K. S.; Özyilmaz, B.; Ahn, J.-H.; Hong, B. H.; Iijima, S. *Nat. Nanotechnol.* **2010**, *5*, 574. doi:10.1038/nnano.2010.132.
(13) Obraztsov, A. N.; Obraztsova, E. A.; Tyurnina, A. V.; Zolotukhin, A. A. *Carbon* **2007**, *45*, 2017. doi:10.1016/j.carbon.2007.05.028.
(14) Wang, J. J.; Zhu, M. Y.; Outlaw, R. A.; Zhao, X.; Manos, D. M.; Holloway, B. C.; Mammana, V. P. *Appl. Phys. Lett.* **2004**, *85*, 1265. doi:10.1063/1.1782253.

(15) Zhu, M.; Wang, J.; Outlaw, R. A.; Hou, K.; Manos, D. M.; Holloway, B. C. *Diam. Relat. Mater.* **2007**, *16*, 196. doi:10.1016/j.diamond.2006.05.007.
(16) Kelly, P. J.; Arnell, R. D. *Vacuum* **2000**, *56*, 159. doi:10.1016/S0042-207X(99)00189-X.
(17) Shih, W.-C.; Jeng, J.-M.; Lo, J.-T.; Chen, H.-C.; Lin, I.-N. *J. Mater. Sci. Mater. Electron.* **2010**, *21*, 926. doi:10.1007/s10854-009-0019-9.
(18) Shih, W.-C.; Jeng, J.-M.; Huang, C.-T.; Lo, J.-T. *Vacuum* **2010**, *84*, 1452. doi:10.1016/j.vacuum.2010.01.049.
(19) Deng, J.; Zheng, R.; Zhao, Y.; Cheng, G. *ACS Nano* **2012**, *6*, 3727. doi:10.1021/nn300900v.
(20) Yurkov, A. N.; Melnik, N. N.; Sychev, V. V.; Savranskii, V. V.; Vlasov, D. V.; Konov, V. I. *Bull. Lebedev Phys. Inst.* **2011**, *38*, 263. doi:10.3103/S106833561109003X.
(21) Yoo, J. J.; Balakrishnan, K.; Huang, J.; Meunier, V.; Sumpter, B. G.; Srivastava, A.; Conway, M.; Mohana Reddy, A. L.; Yu, J.; Vajtai, R.; Ajayan, P. M. *Nano Lett.* **2011**, *11*, 1423. doi:10.1021/nl200225j.
(22) Wu, Y.; Qiao, P.; Chong, T.; Shen, Z. *Adv. Mater.* **2002**, *14*, 64. doi:10.1002/1521-4095(20020104)14:1<64::AID-ADMA64>3.0.CO;2-G.
(23) Shiji, K.; Hiramatsu, M.; Enomoto, A.; Nakamura, M.; Amano, H.; Hori, M. *Diam. Relat. Mater.* **2005**, *14*, 831. doi:10.1016/j.diamond.2004.10.021.
(24) Ferrari, A. C.; Robertson, J. *Phys. Rev. B* **2000**, *61*, 14095. doi:10.1103/PhysRevB.61.14095.
(25) Wang, J.; Zhu, M.; Outlaw, R. A.; Zhao, X.; Manos, D. M.; Holloway, B. C. *Carbon* **2004**, *42*, 2867. doi:10.1016/j.carbon.2004.06.035.
(26) Cuesta, A.; Dhamelincourt, P.; Laureyns, J.; Martínez-Alonso, A.; Tascón, J. M. D. *Carbon* **1994**, *32*, 1523. doi:10.1016/0008-6223(94)90148-1.
(27) Ferrari, A. C.; Meyer, J. C.; Scardaci, V.; Casiraghi, C.; Lazzeri, M.; Mauri, F.; Piscanec, S.; Jiang, D.; Novoselov, K. S.; Roth, S.; Geim, A. K. *Phys. Rev. Lett.* **2006**, *97*, 187401. doi:10.1103/PhysRevLett.97.187401.
(28) Losurdo, M.; Giangregorio, M. M.; Capezzuto, P.; Bruno, G. *Phys. Chem. Chem. Phys.* **2011**, *13*, 20836. doi:10.1039/c1cp22347j.
(29) Hiramatsu, M.; Shiji, K.; Amano, H.; Hori, M. *Appl. Phys. Lett.* **2004**, *84*, 4708. doi:10.1063/1.1762702.
(30) Mucha, J. A.; Flamm, D. L.; Ibbotson, D. E. *J. Appl. Phys.* **1989**, *65*, 3448. doi:10.1063/1.342635.
(31) Muranaka, Y.; Yamashita, H.; Sato, K.; Miyadera, H. *J. Appl. Phys.* **1990**, *67*, 6247. doi:10.1063/1.345191.
(32) Stankovich, S.; Dikin, D. A.; Piner, R. D.; Kohlhaas, K. A.; Kleinhammes, A.; Jia, Y.; Wu, Y.; Nguyen, S. T.; Ruoff, R. S. *Carbon* **2007**, *45*, 1558. doi:10.1016/j.carbon.2007.02.034.
(33) Yan, J.; Liu, J.; Fan, Z.; Wei, T.; Zhang, L. *Carbon* **2012**, *50*, 2179. doi:10.1016/j.carbon.2012.01.028.
(34) Cao, H.; Zhou, X.; Qin, Z.; Liu, Z. *Carbon* **2013**, *56*, 218. doi:10.1016/j.carbon.2013.01.005.